Periodic forcing of a limit-cycle oscillator: Fixed points, Arnold tongues, and the global organization of bifurcations

Leon Glass and Jiong Sun

Department of Physiology, McGill University, 3655 Drummond Street, Montreal, Quebec, Canada H3G 1Y6

(Received 12 August 1994)

The effects of periodic pulsatile stimuli on a nonlinear limit-cycle oscillation are analyzed for various relaxation rates to the limit-cycle oscillation. In the infinite relaxation limit, the effects of periodic stimuli are analyzed by consideration of the bifurcations of circle maps. In the case of a finite relaxation rate, it is necessary to analyze two-dimensional maps of the disk. However, the simple structure of the limit cycle allows us to carry out detailed theoretical and numerical analyses of the dynamics. Using the Brouwer fixed point theorem, we show that for any finite nonzero frequency and amplitude of the stimulus, there will be a period-1 fixed point associated with a period-1 phase locking. We use analytical and numerical methods to determine the stability boundary of the period-1 fixed point as a function of the stimulation frequency, amplitude, and relaxation rate to the limit cycle. These results, combined with numerical studies give insight into the changes in the global organization of the phase locking zones as a function of the relaxation rate to the limit cycle.

PACS number(s): 87.22.As, 02.30.Hq, 05.45.+b

I. INTRODUCTION

The periodic forcing of nonlinear oscillators has been a topic of broad interest to basic scientists, engineers, and mathematicians [1–10]. Recent years have witnessed progress in understanding the organization of the zones of entrainment combining numerical and analytical methods on simplified theoretical models, and in different experimental settings [11–20].

Our own interest in periodically forced oscillators stems from their importance in biology [16]. Extensive experimental and theoretical studies of the effects of periodic pulsatile stimulation of cardiac oscillators have demonstrated that to a first approximation, experimental results can be modeled by the iteration of one-dimensional circle maps $g : S^1 \to S^1$. The essential assumptions in deriving this approximation are (i) the oscillator is modeled by a limit-cycle attractor; (ii) the time interval between stimulations is sufficiently long that the oscillator returns to the limit cycle between stimuli; and (iii) the stimulation does not change the properties of the limit cycle. The mathematical analysis of the dynamics arising from iteration of one-dimensional circle maps helps to explain the origin of complex rhythms and aperiodic rhythms that are experimentally observed during periodic stimulation, and gives a good understanding of the global organization of the dynamics as a function of stimulus frequency and amplitude [16].

However, recent experimental studies indicate limitations of this approach. For example, if periodic stimuli are delivered too close together in time, then the trajectory does not return to the limit cycle between stimuli and a one-dimensional circle map can no longer be applied to compute the effects of repeated stimulation [21]. Assuming that the limit-cycle oscillation is generated by a two-dimensional differential equation, then the dynamics will be described by maps of the plane. There is a broad mathematical literature analyzing the dynamics arising from iteration of such maps, including extensive studies of the problem of periodically forced nonlinear oscillations [11–15]. Despite these advances, there is still not a clear understanding of the global organization of phase locking zones.

Our approach to this problem is to consider dynamics in what we believe is the simplest theoretical model of a periodically forced two-dimensional limit-cycle oscillator [17–20]. This theoretical model, in which the limit-cycle attractor is a circle in a two-dimensional phase space [9], has been extensively studied under a variety of names (radial isochron clock [18], λ-ω system [22], Poincaré oscillator [10]). In view of the relative obscurity of the first two names, and the fact that Poincaré was the first to consider phase planes with this geometry, we prefer the term Poincaré oscillator.

In Sec. II we introduce the theoretical model and define terms used to characterize the dynamics. In Sec. III we summarize the main results found previously for the "infinite relaxation limit" in which the periodic forcing is described by one-dimensional circle maps. Sections IV and V give an analysis of the period-1 fixed point during periodic stimulation. Section IV applies the Brouwer fixed point theorem to prove that for any values of stimulation and frequency there exists a period-1 fixed point for the Poincaré oscillator, and Section V develops numerical formulas to compute the period-1 fixed points and evaluate their stability. Section VI gives additional numerical analysis of the global structure of the dynamics as a function of the stimulus frequency and amplitude.

II. THE PERIODICALLY FORCED POINCARÉ OSCILLATOR–BASIC EQUATIONS AND DEFINITIONS

The Poincaré oscillator [9, 10, 17, 18] is most conveniently written in a radial coordinate system where r is

the distance from the origin and ϕ is the angular coordinate. The equations are written

$$\frac{dr}{dt} = kr(1-r),$$
$$\frac{d\phi}{dt} = 1, \tag{2.1}$$

where k is a positive parameter and ϕ is a normalized angular coordinate varying in the interval [0,1) corresponding to $[0, 2\pi)$ radians [17, 19]. By rescaling the time t and the constant k, we can always make the right hand side of (2.1) equal to unity without any loss of generality. Starting at any value of r, except for $r = 0$, there is an evolution until $r = 1$. The parameter k controls the relaxation rate to the limit cycle.

We call $\phi = 0$ the fiducial point of the cycle associated with the start of the cycle. We model the stimulation of the Poincaré oscillator by an instantaneous horizontal translation by an amount b, Fig. 1. Assume that immediately before stimulus i, we are at a point (r_i, ϕ_i). The stimulus takes us from the point (r_i, ϕ_i) to point (r_i', ϕ_i'), where

$$r_i' = [r_i^2 + b^2 + 2br_i \cos(2\pi\phi_i)]^{1/2},$$
$$\phi_i' = \frac{1}{2\pi} \arccos \frac{r_i \cos(2\pi\phi_i) + b}{r_i'}. \tag{2.2}$$

In computations using Eq. (2.2), in evaluating the arccosine function, we must take $0 < \phi_i' < 0.5$ for $0 < \phi_i < 0.5$, and $0.5 < \phi_i' < 1$ for $0.5 < \phi_i < 1$. Following the stimulus, the equations of motion (2.1) take over, so that by direct integration, we find that immediately before stimulus $(i+1)$ delivered at a time τ after the first stimulus, we have

$$r_{i+1} = \frac{r_i'}{(1-r_i')\exp(-k\tau) + r_i'},$$
$$\phi_{i+1} = \phi_i' + \tau (\text{mod } 1). \tag{2.3}$$

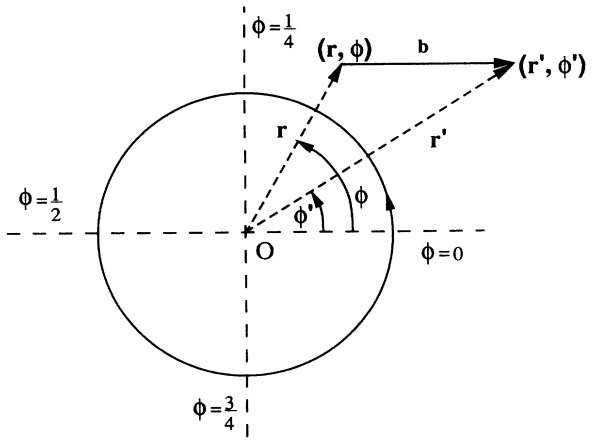

FIG. 1. The effect of perturbation of the Poincaré oscillator. The point (r, ϕ) is sent to point (r', ϕ') by the stimulus. There is a stable limit-cycle attractor at $r = 1$. We scale the angular coordinate to lie between 0 and 1, and take the fiducial point of the cycle as $\phi = 0$. The perturbation is a horizontal translation b.

The remainder of this paper deals with the properties of the periodically forced Poincaré oscillator based on iteration of Eq. (2.3).

Starting from an initial condition (r_0, ϕ_0) we generate the sequence of points (r_1, ϕ_1), $(r_2, \phi_2), \ldots$. A *periodic orbit* of period n is present if $r_{i+n} = r_i$, $\phi_{i+n} = \phi_i$ provided $r_{i+k} \neq r_i$, $\phi_{i+k} \neq \phi_i$ for $1 \leq k < n$.

The *rotation number*, ρ, gives the average increase in ϕ per iteration. Calling

$$\Delta_{i+1} = \phi_i' + \tau - \phi_i, \tag{2.4}$$

we have

$$\rho = \limsup_{N\to\infty} \frac{1}{N} \sum_{i=1}^{N} \Delta_i. \tag{2.5}$$

Periodic orbits are associated with *phase locking*. In $n : m$ phase locking, there is a periodic orbit consisting of n stimuli and m cycles of the oscillator leading to a rotation number m/n. For periodically forced oscillators neither the periodicity nor the rotation number alone is adequate to characterize the dynamics.

In order to analyze the stability of a periodic orbit of period n, it is necessary to compute the Jacobian matrix, M_i, defined by

$$M_i = \begin{pmatrix} A_i & B_i \\ C_i & D_i \end{pmatrix}, \tag{2.6}$$

where $A_i = \frac{\partial\phi_{i+1}}{\partial\phi_i}$, $B_i = \frac{\partial\phi_{i+1}}{\partial r_i}$, $C_i = \frac{\partial r_{i+1}}{\partial\phi_i}$, $D_i = \frac{\partial r_{i+1}}{\partial r_i}$. The computation of the partial derivatives leads to the following algebraic expressions:

$$A_i = \frac{r_i^2 + br_i \cos(2\pi\phi_i)}{(r_i')^2},$$

$$B_i = \frac{b \sin(2\pi\phi_i)}{2\pi(r_i')^2}$$

$$C_i = \frac{-[2\pi br_i \sin(2\pi\phi_i)]e^{-k\tau}}{r_i'[(1-r_i')e^{-k\tau} + r_i']^2},$$

$$D_i = \frac{[r_i + b\cos(2\pi\phi_i)]e^{-k\tau}}{r_i'[(1-r_i')e^{-k\tau} + r_i']^2},$$

where (r_i, ϕ_i) are the coordinates of a point of the period n cycle. During periodic stimulation, the stability of a periodic cycle of period n is given by the eigenvalues of the matrix

$$M = \prod_{i=1}^{n} M_i. \tag{2.7}$$

If the eigenvalues lie within the unit circle then there is a stable periodic orbit.

III. THE INFINITE RELAXATION LIMIT

There are several papers studying the effects of periodic stimulation of the Poincaré oscillator in the infinite relaxation limit, $k \to \infty$ [17–20]. We very briefly review this work. A schematic diagram illustrating some of the

main phase locking regions is shown in Fig. 2 adapted from Refs. [17, 19].

In the infinite relaxation limit, the dynamics are described by a one-dimensional circle map $g : S^1 \to S^1$,

$$\phi_{i+1} = g(\phi_i) + \tau \tag{3.1}$$

that is found from Eq. (2.3) by taking the limit $k \to \infty$. The *topological degree* of a circle map counts the number of times the map winds around the circle as the variable goes around the circle once. For $0 \leq b < 1$ the map is of topological degree 1 and for $1 < b$, the map is of topological degree 0. The bifurcations that are displayed by this problem are consequently typical of bifurcations that are found in studies of the bifurcations in circle maps with two parameters. There are complications, however, associated with the joining of the zones where the map changes its topological degree near $b = 1$.

$0 \leq b < 1$. The map is an invertible diffeomorphism of the circle. An *Arnold tongue of rotation number* m/n of a circle map is defined as the union of values in parameter space for which there exists periodic solution with rotation number m/n [7, 8]. For invertible diffeomorphisms of the circle, the case initially considered by Arnold, for a fixed set of parameters, all initial conditions have the same rotation number. Moreover, if there is $n : m$ phase locking for τ and $n' : m'$ phase locking for τ', then there exists a value τ^*, $\tau < \tau^* < \tau'$, leading to $n + n' : m + m'$ phase locking. Usually, the range of values of τ associated with a given Arnold tongue covers an open interval in parameter space. If the rotation number is rational, there is phase locking, and if the rotation number is irrational there is *quasiperiodicity*. The organization of phase locking zones for $0 \leq b < 1$ shown in Fig. 2 is typical, and is called the *classic Arnold tongue structure*. The periodic orbits lose stability via a tangent bifurcation.

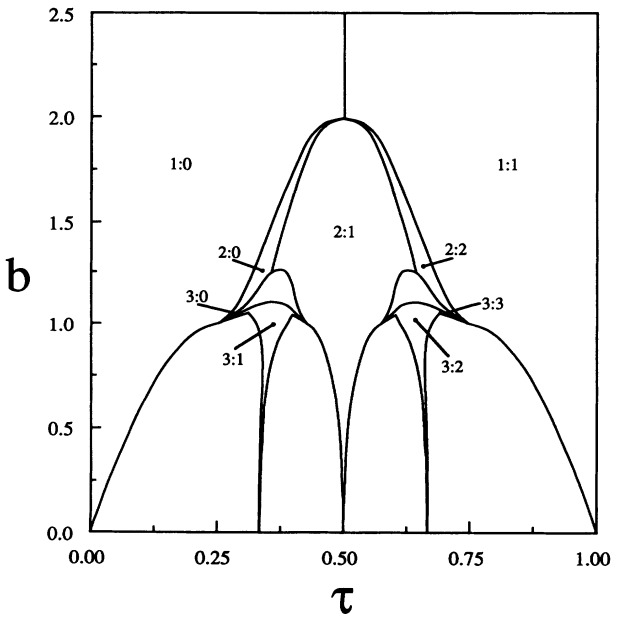

FIG. 2. The parameter space in the infinite relaxation $k \to \infty$ limit showing the different phase locking zones. Modified from [17, 19].

$1 < b$. The map now has two local extrema. For any set of parameter values there is no longer necessarily a unique attractor. It is possible to have *bistability* in which there exist two stable attractors for a given set of parameter values. The attractors are either periodic or chaotic. A *superstable cycle* is a cycle containing a local extremum. Such cycles are guaranteed to be stable. One way to get a good geometric picture of the structure of the zones is to plot the locus of the superstable cycles in the parameter space [19]. As b decreases in this zone, new phase locking zones arise; however, almost all these zones disappear into the discontinuities of the circle map at $b = 1$.

In previous work [19] the intersection of the Arnold tongues with the line $b = 1$ was considered. Numerical studies showed that the intersection points of the Arnold tongues with the line $b = 1$ were accumulation points of superstable orbits. It was proven that the endpoint of a period k phase locked region is the terminus of a period j superstable orbits for every $j \geq k$. Therefore, the junctions of the Arnold tongues with the line $b = 1$ represent accumulation points of an infinite number of phase locking zones. For example, the point in Fig. 2 at $b = 1$, $\tau = 0.25$, is an accumulation point of an infinite number of superstable cycles including superstable cycles originating at the right boundary of the the intersection of the 5:1, 4:1, 3:1, 2:1 Arnold tongues with the line $b = 1$, see Fig. 5(a) in [19].

The accumulation points of stable phase locking zones at the intersection of the Arnold tongues with the line $b = 1$ are subtle geometrical features of the structure of the phase locking regions in the periodic forcing amplitude and frequency parameter space that are easily missed in numerical studies. We are not aware of similar features in other theoretical models of periodically forced oscillators. For Eq. (2.3) with the relaxation rate k very large but finite, the geometry must be very similar to the $k \to \infty$ limit. A conjecture on the way the geometry for the $k \to \infty$ limit, Fig. 2, changes (continuously) for k large but finite is presented in Sec. VI.

The period-1 cycle (fixed point) loses stability by a period doubling bifurcation for $1 < b < 2$. In this problem there can be changes in the rotation number without a change in periodicity [17]. Thus for $2 < b$, there is a change from 1:0 phase locking to 1:1 phase locking along the line $\tau = 0.5$.

In the infinite relaxation limit there are important symmetry relations that are evident in Fig. 2. These symmetry relations are derived in [17], which should be consulted for details.

Symmetry 1. Assume that there is a stable period-n cycle with fixed points $\phi_0, \phi_1, \ldots, \phi_{n-1}$ for $\tau = 0.5 - \delta$, $0 < \delta < 0.5$, associated with $n : m$ phase locking. Then for $\tau = 0.5 + \delta$, there will be a stable cycle of period n associated with an $n : n - m$ phase locking ratio. The n fixed points are $\psi_0, \psi_1, \ldots, \psi_{n-1}$ where $\psi_i = 1 - \phi_i$.

Symmetry 2. Assume that there is a stable period-n cycle with fixed points are $\phi_0, \phi_1, \ldots, \phi_{n-1}$ for $\tau = \delta$, $0 < \delta < 1.0$, associated with $n : m$ phase locking.

$\tau = \delta + k$, where k is a positive integer, there will be a stable cycle of period n associated with an $n : m + nk$ phase locking ratio. The n fixed points are $\psi_0, \psi_1, \ldots, \psi_{n-1}$ where $\psi_i = \phi_i$.

Symmetry 1 is satisfied in Fig. 2. Using the translational symmetry, symmetry 2, the zones in Fig. 2 can be expanded to cover the region $\tau > 1$.

IV. EXISTENCE PROOF FOR PERIOD-1 CYCLE

The *Brouwer fixed point theorem* [23] states that any continuous function f of the closed disk $D^n \subset R^n$ into itself must have a fixed point; that is, $f(x) = x$ for some $x \in D^n$.

In the current case, the two-dimensional map, given by Eqs. (2.2) and (2.3) is generated by integration of continuous differential equations, so that continuity of the map is ensured.

Consider a disk D of radius R_m in the two-dimensional phase space centered at the origin, Fig. 3(a). The perturbation leads to a horizontal displacement of each point in D by b, leading to D', Fig. 3(b). If the disk is of radius R_m, then the point $(R_m, 0)$ suffers the furthest displacement from D under the stimulation. However, a simple computation lets us determine the value of R_m that guarantees that D maps into itself. We use Eq. (2.3) to compute the evolution of $(R_m, 0)$ following a horizontal perturbation b after a time τ. For any given values of b, k, and τ, D will be mapped into itself provided

$$R_m \geq R_{\text{crit}} = \frac{|1-b|}{2} + \frac{1}{2}\sqrt{(1-b)^2 + \frac{4b}{1-e^{-k\tau}}}, \quad (4.1)$$

where R_{crit} is the minimum radius such that $f(D) \in D$, where f represents the two-dimensional map in (2.3). Figure 3(c) shows the situation that prevails with $b = 0.8$, $k = 1.0$, $\tau = 0.3$ yielding $R_{\text{crit}} \approx 1.86$. Since D maps into itself, the Brouwer fixed point theorem is applicable. We therefore have proven the following theorem.

Theorem. For the 2 dimensional Poincaré oscillator, Eq. (2.1), subjected to a periodic pulsatile stimulus, there will be a period-1 cycle for any amplitude or frequency of the periodic forcing.

This represents an important difference from the infinite relaxation limit in Sec. III. In the infinite relaxation limit, for $0 < b < 1$, inside the Arnold tongues associated with $n : m$ locking with $n > 1$, there is not a fixed point of period-1. Notice, however, that the period-1 cycle that must exist in the finite relaxation limit is not necessarily stable.

Although, this result has been derived for the particular case of the periodically forced Poincaré oscillator, it will likewise be applicable for periodic forcing of any limit cycle oscillation in finite dimensions provided the magnitude of the inward flow towards the limit cycle contained in D^n grows sufficiently rapidly as the disk radius increases. In the same way, excitable (nonoscillating) systems [9, 10] subjected to periodic forcing should also display period-1 cycles, if similar restrictions apply to the vector field. Because of its broad implications in a variety of systems, this result is one of the main findings of the current paper.

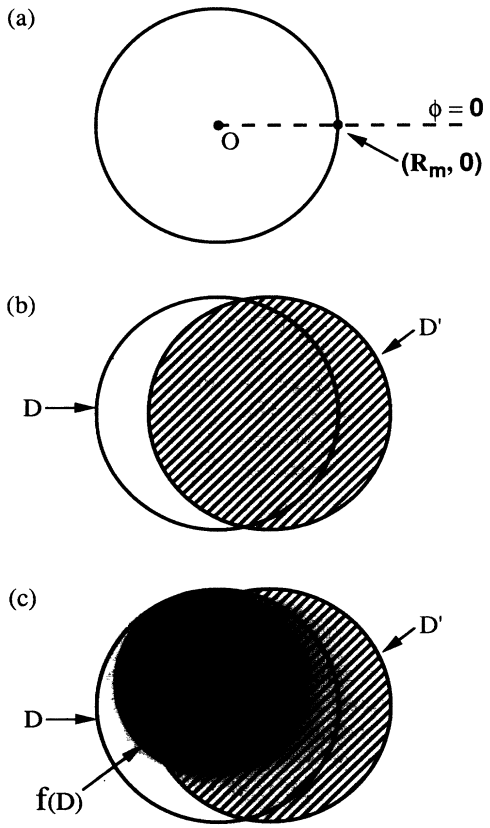

FIG. 3. Schematic diagram showing application of the Brouwer fixed point theorem to prove existence of a period-1 fixed point illustrated for the case $b = 0.8, k = 1.0, \tau = 0.3$. (a) The initial disk D of radius $R_m \approx 1.86$, centered at the origin. (b) D is mapped to a new disk D' by the perturbation of a horizontal translation b. (c) After time τ has elapsed, D evolves to $f(D)$, where $f(D) \in D$.

V. ANALYSIS OF 1:M LOCKING

A. Computation of the fixed point

A fixed point (r_0, ϕ_0) in Eq. (2.3) corresponds to a $1 : m$ locking rhythm, where, using Eq. (2.4), $m = \Delta_0$. This section shows how the fixed points and their stability can be determined numerically. Figure 4 shows a typical situation associated with a fixed point. We call the fixed point (r_0, ϕ_0). Under the perturbation b this point is mapped to the point (r', ϕ') where $\phi' = \phi_0 - \tau$. Using the law of sines, we calculate

$$\frac{\sin(2\pi\phi_0)}{r'} = \frac{\sin(2\pi\tau)}{b} = \frac{\sin[2\pi(\phi_0 - \tau)]}{r_0}. \quad (5.1)$$

We develop a transcendental equation to solve for ϕ_0. From Eqs. (2.3) and (5.1), we compute

$$r_0 = \frac{r'}{(1-r')e^{-k\tau} + r'} = \frac{b\,\sin[2\pi(\phi_0 - \tau)]}{\sin(2\pi\tau)} \quad (5.2)$$

Substituting, for r' from Eq. (5.1), we can equate the

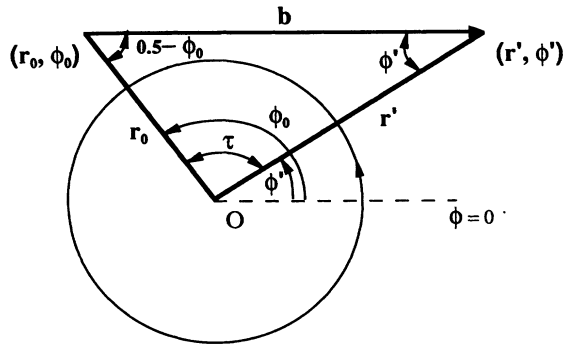

FIG. 4. Schematic diagram showing the geometry underlying the computation of the period-1 fixed point.

two equivalent expressions for r_0 in Eq. (5.2) to obtain the equation

$$b\sin[2\pi(\phi_0-\tau)] = \left(\frac{e^{-k\tau}\sin^2(2\pi\tau)}{1-e^{-k\tau}}\right)\cot(2\pi\phi_0) + \left(\frac{1-e^{-k\tau}\cos(2\pi\tau)}{1-e^{-k\tau}}\right)\sin(2\pi\tau), \tag{5.3}$$

where the only roots of interest lie in the range $0<\phi_0<0.5$ for $0<\tau \pmod 1<0.5$ and $0.5<\phi_0<1$ for $0.5<\tau \pmod 1<1$. From the mean value theorem, at least one solution of this equation will always exist for any values of b, k, τ. For large values of the product of $k\tau$, one solution will always be found in the neighborhood of singular values of the cotangent function at $\phi_0=0$ or $\phi_0=0.5$. Once ϕ_0 is determined, we can compute r_0 using Eq. (5.1).

B. Stability of the fixed point

The computation of the stability of the fixed point follows from the definition of the Jacobian matrix in Sec. II. Calling

$$L_1 = (A_i+B_i)|_{(r_0,\phi_0)},$$
$$L_2 = (A_iD_i-B_iC_i)|_{(r_0,\phi_0)}$$

from (2.6), we find that

$$L_1 = S\cos 2\pi\tau(1+Se^{-k\tau}),$$
$$L_2 = S^3e^{-k\tau}, \tag{5.4}$$

where $S=r_0/r'$.

The eigenvalues are found by solving the equation

$$\lambda^2 - L_1\lambda + L_2 = 0. \tag{5.5}$$

Solving this equation for λ we compute

$$\lambda = \frac{S(1+Se^{-k\tau})}{2}\left[\cos(2\pi\tau) \pm \sqrt{y^2-\sin^2(2\pi\tau)}\right], \tag{5.6}$$

where

$$y = \frac{1-Se^{-k\tau}}{1+Se^{-k\tau}}.$$

C. Infinite relaxation limit

The stability of the period-1 solution for the infinite relaxation limit $k\to\infty$, has been given in previous papers [17, 18, 20]. The boundaries also follow as a special case from the formulas developed for the two-dimensional case. For completeness, we summarize these results (with some simplifications), and refer the reader to earlier papers for more details.

In the strong relaxation limit we have $r_0=1$. For $0<b<1$ the stability is lost by a tangent bifurcation for which $\frac{\partial\phi_{i+1}}{\partial\phi_i}=1$. This implies that at the boundary we have

$$b+\cos(2\pi\phi_0)=0,$$

from which we compute

$$b = |\sin(2\pi\tau)|. \tag{5.7}$$

The fixed point at the stability boundary is at

$$\phi_0 = \tau+\frac{1}{4}, \text{ for } 0<\tau<\frac{1}{4},$$

and

$$\phi_0 = \tau+\frac{3}{4}, \text{ for } \frac{3}{4}<\tau<1.$$

For $1<b<2$ stability of the period-1 fixed point is lost by a period doubling bifurcation for which $\frac{\partial\phi_{i+1}}{\partial\phi_i}=-1$. From this we compute that at the boundary we have

$$2+b^2+3b\cos(2\pi\phi_0)=0.$$

Carrying through the trigonometry we find the stability boundary

$$b = \sqrt{4-3\sin^2(2\pi\tau)}. \tag{5.8}$$

The fixed point at the boundary is given by

$$\phi_0 = \tau+\frac{1}{2\pi}\sin^{-1}\sqrt{\frac{4-b^2}{3b^2}}.$$

D. Weak relaxation limit

In the weak relaxation limit, $k\to 0$, and we find $r_0=r'$, $S=1$, $y=0$. For this case there is a solution

$$\phi_0 = 0.25+\tau/2,$$
$$r_0 = \frac{b}{2\sin\pi\tau} \tag{5.9}$$

for $0<\tau \pmod 1<1.0$. The eigenvalues for this solution are

$$\lambda = e^{\pm 2\pi i\tau}. \tag{5.10}$$

Since the eigenvalues in the limit $k\to 0$ lie on the unit circle, it is necessary to analyze the stability by considering the power expansion of the modulus as $k\to 0$. When the eigenvalues are complex conjugates, the modulus is equal to L_2 in (5.4). From (5.2) and (5.4) we find that

$$L_2 = (r_0/r')^3 e^{-k\tau} \approx \frac{1-k\tau}{1-3k\tau(1-r')} \approx 1 + 2k\tau - 3k\tau r' + \cdots . \tag{5.11}$$

Therefore, if $r' > \frac{2}{3}$ the period-1 solution is stable. Otherwise it is unstable. From (5.9) we now compute that the period-1 solution is stable if

$$b > \frac{4}{3}\sin \pi\tau. \tag{5.12}$$

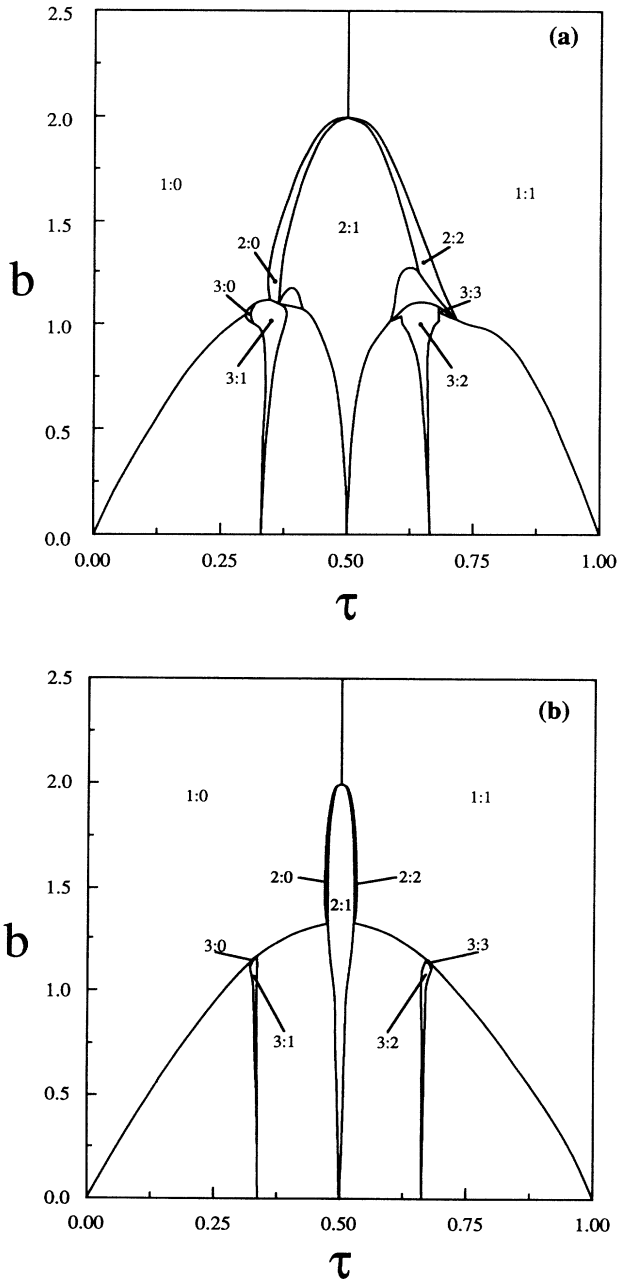

FIG. 5. (a) Numerical computation of the phase locking zones for $k = 10$. (b) Numerical computation of the phase locking zones for $k = 1$.

VI. NUMERICAL STUDIES

Given the initial condition (r_0, ϕ_0), Eqs. (2.2) and (2.3) were iterated to generate the sequence (r_1, ϕ_1), (r_2, ϕ_2), ..., (r_n, ϕ_n). Periodic cycles were determined after allowing a sufficiently long transient that asymptotic behavior is achieved. The boundaries of the different locking zones are automatically detected. The computations were carried out on a SunSparc Workstation using double precision.

One of the numerical difficulties in these computations is the effect of initial conditions. For some parameter values the rhythm is not uniquely determined but depends on the initial conditions. For example, at $k = 10$, $b = 1.08$, and $\tau = 0.306$ we have found two different stable rhythms. For $r_0 = 0.91$, $\phi_0 = 0.45$, the rhythm evolves to a 1:0 rhythm, while for $r_0 = 1.0$, $\phi_0 = 0.3$, the rhythm evolves to a 3:0 rhythm. In numerical studies in the infinite relaxation limit it is possible to track superstable orbits, and in this way demonstrate rich bistability for $b > 1$ [19]. In the finite relaxation limit we do not know of an analogous numerical trick. In view of the extremely small basins of attraction expected for some of the locking zones, and the expected complex topology of these multistable zones, we have not carried out a detailed numerical study of multistability. In this study, we arbitrarily fixed the initial condition to be $r_0 = 1.0$ and $\phi_0 = 0.3$. Since we expect multistability, diagrams of phase locking zones assuming a different initial condition would show differences, but these do not affect the major conclusions of the current analysis.

Figure 5 shows the phase locking zones for $k = 10$ and $k = 1$. These should be compared with the $k \to \infty$ diagram in Fig. 2 [19]. With finite relaxation, the phase locking zones become narrower in size. For example the 2:1 phase locking zone shrinks dramatically when k becomes small. The reflection symmetry around $\tau = 0.5$ is

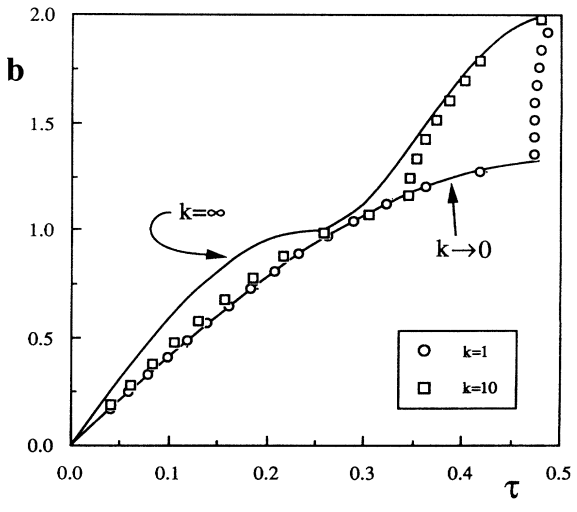

FIG. 6. Period-1 boundary for several values of k. The results for $k \to \infty$ and $k \to 0$ are based on the analytical formula in the text, and the values for $k = 10$ and $k = 1$ are based on the numerical computations.

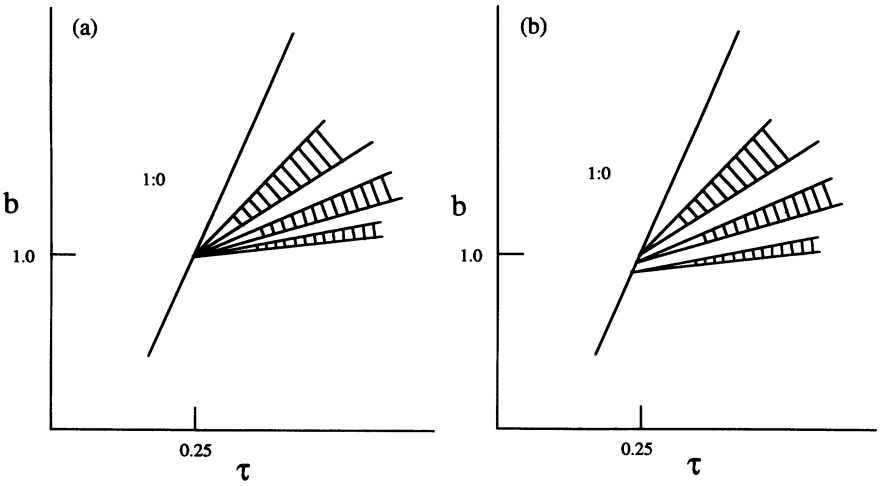

FIG. 7. (a) Schematic diagram of the geometry in the neighborhood of the point $b = 1$, $\tau = 0.25$ for the infinite relaxation limit $k \to \infty$. Based on results in [17, 19]. (b) Conjectured diagram of the geometry in the neighborhood of the point $b = 1$, $\tau = 0.25$ for k large but finite. Similar geometries should be observed in the neighborhood of the intersection of each Arnold tongue with the line $b = 1$.

lost for positive finite k but is reestablished in the $k \to 0$ limit.

We now turn to delicate questions concerning the 1:0 boundary. In Fig. 6, we plot the 1:0 boundaries for $k \to 0$, $k = 1$, $k = 10$, and $k \to \infty$. The boundaries are obtained from theoretical formula for $k \to \infty$ [Eqs. (5.7) and (5.8)], and $k \to 0$ [Eq. (5.12)]. The boundaries are obtained numerically for $k = 1$ and $k = 10$.

For $k \to \infty$ the nature of the bifurcation on the boundary is understood. For $0 < b < 1$, $0 < \tau < 0.25$ there is a tangent bifurcation, and for $1 < b < 2$, $0.25 < \tau < 0.5$, there is a period doubling boundary, see Sec. V C. The point $b = 1$, $\tau = 0.25$ is a singular point that represents the intersection of the 1:0 locking zone with the line $b = 1$. As discussed in Sec. III, this point is an accumulation point of an infinite number of superstable cycles. This is represented schematically in Fig. 7(a).

We now consider the way this geometry is modified in the finite k limit. We determine the period-1 orbit numerically and evaluate the eigenvalues to analyze the loss of stability for fixed b as τ increases, Fig. 8. The loss of stability is through a Hopf bifurcation (two complex eigenvalues lie on the unit circle) or a period doubling bifurcation (both eigenvalues are real and one is equal to -1). As b increases over the range of parameter values that lead to the Hopf bifurcation, the eigenvalues traverse the unit circle. We call the angular coordinate of the eigenvalues in the complex plane, θ_λ, where $\theta_\lambda = 0$ corresponds to both eigenvalues equal to 1, and $\theta_\lambda = 0.5$ corresponds to both eigenvalues equal to -1 (see the inset in Fig. 8). Our numerical studies indicate that at $b = 0$ both eigenvalues lie at $\theta_\lambda = 0$. These traverse the unit circle as b increases until there is a period doubling bifurcation for $b_{\max}(k)$, Fig. 8. This picture suggests that the accumulation point of superstable cycles at $b = 1, \tau = 0.25$ is destroyed in a natural way for k large but finite to yield the generic picture of Arnold tongues in two-dimensional maps. Figure 7(b) is a conjectured organization of the locking zones near $b = 1$, $\tau = 0.25$ for finite large k. This should be compared with Fig. 153 in [7]. We conjecture that the geometry in Fig. 7(b) is repeated at the intersections of other Arnold tongues with $b = 1$ for k large but finite. As k further decreases the cusps smooth out and the locking zones continuously evolve to the $k \to 0$ limit, Fig. 5(b). Intermediate stages are superficially similar to reported organization of locking zones in many other articles.

VII. DISCUSSION

The current paper has considered dynamics in a theoretical model of a periodically forced limit-cycle oscillation as a function of both the frequency and amplitude of the periodic forcing. The equation is probably the simplest imaginable displaying a stable limit cycle, and dates back to Poincaré. The equation, or simple variants of it, has been independently proposed by many differ-

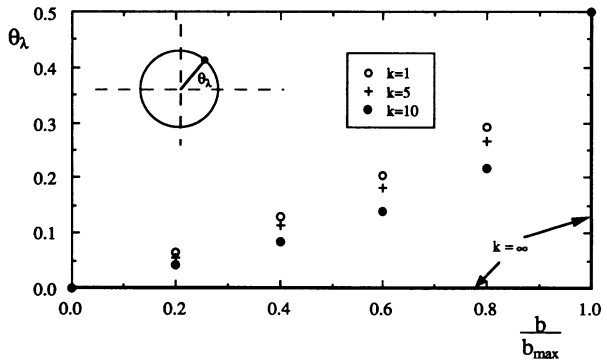

FIG. 8. The locus of the eigenvalues at the loss of stability of the period-1 orbit as a function of b. Computed from numerical solution of the transcendental equation (5.3) to determine the fixed point, and evaluation of (5.5) to evaluate the eigenvalues. For $0 < b < b_{\max}(k)$ the eigenvalues lie on the unit circle, and stability is lost via a Hopf bifurcation. The location of the eigenvalues on the unit circle is given by θ_λ as shown in the inset. For $b > b_{\max}(k)$ stability is lost via a period doubling bifurcation so that at the instability one eigenvalue is -1. For $k \to 0$, $k = 1$, $k = 10$, $k \to \infty$, respectively, the values of $b_{\max}(k)$ are 4/3, ≈ 1.32, ≈ 1.12, 1.0, respectively.

ent investigators, sometimes unaware of earlier research [17–20]. This prototypical example captures many basic properities of periodically forced limit-cycle oscillations and as such it deserves to be better known and appreciated. Previous studies examined dynamics of this equation in a limit of strong relaxation, in which the trajectories are attracted to the limit cycle infinitely fast [17–20]. We are not aware of studies involving the finite relaxation limit.

For any stimulation frequency and amplitude there exists a period-1 fixed point. This has important implications for our understanding of Arnold tongues for periodically forced two-dimensional limit-cycle oscillators. The lack of uniqueness of rotation number inside the Arnold tongue, even for small amplitude forcing is a novel feature in this, and undoubtedly many other systems.

Because of the simplicity of the model, analytic results concerning the stability of the period-1 boundary have been possible. However, there remain a large number of additional questions that have not been addressed. For example, is the Hopf bifurcation subcritical or supercritical along the period-1 boundary? More difficult questions involve the global organization of the locking zones for finite k. We have conjectured that singular accumulation points of superstable cycles in the $k \to \infty$ limit are destroyed in a natural way for finite k. However, the detailed evolution of the global organization of locking zones as k decreases is still not clear.

ACKNOWLEDGMENTS

This research has been partially supported by funds from the Natural Sciences Engineering and Research Council and the Canadian Heart and Stroke Association.

[1] C. Hayashi, *Nonlinear Oscillations in Physical Systems* (McGraw-Hill, New York, 1964).
[2] K. Tomita and T. Kai, J. Stat. Phys. **21**, 65 (1979).
[3] P. S. Linsay, Phys. Rev. Lett. **47**, 1349 (1981); J. S. Testa, J. Pérez, and C. Jeffries, Phys. Rev. Lett. **48**, 714 (1982).
[4] D. L. Gonzalez and O. Piro, Phys. Rev. Lett. **50**, 870 (1983).
[5] C. Scheffczyk, U. Parlitz, T. Kurz, W. Knop, and W. Lauterborn, Phys. Rev. A. **43**, 6495 (1991).
[6] *Chaos*, edited by A. Holden (Manchester University Press, Manchester, 1986).
[7] V. I. Arnold, *Geometrical Methods in the Theory of Ordinary Differential Equations* (Springer-Verlag, New York, 1983).
[8] J. Guckenheimer and P. Holmes, *Nonlinear Oscillations, Dynamical Systems and Bifurcations of Vector Fields*, 3rd ed. (Springer-Verlag, New York, 1990).
[9] A. T. Winfree, *The Geometry of Biological Time* (Springer-Verlag, New York, 1980).
[10] L. Glass and M. C. Mackey, *From Clocks to Chaos: The Rhythms of Life* (Princeton University Press, Princeton, NJ, 1988).
[11] D. G. Aronson, R. P. McGehee, I. G. Kevrekidis, and R. Aris, Phys. Rev. A **33**, 2190 (1986).
[12] I. Schreiber, M. Doln'ik, P. Choc, and M. Marek, Phys. Lett. A, **128**, 66 (1988).
[13] W. Vance and J. Ross, J. Chem. Phys. **91**, 7654 (1989).
[14] B. B. Peckham, Nonlinearity **3**, 261 (1990).
[15] J. W. Norris, Nonlinearity **6**, 1093 (1993).
[16] M. R. Guevara, L. Glass, and A. Shrier, Science **214**, 1350 (1981); L. Glass, M. R. Guevara, A. Shrier, and R. Perez, Physica **7D**, 89 (1983); L. Glass, M. R. Guevara, J. Bélair, and A. Shrier, Phys. Rev. A **29**, 1348 (1984); W.-Z. Zeng, M. Courtemanche, L. Sehn, A. Shrier, and L. Glass, J. Theor. Biol. **145**, 217 (1990).
[17] M. R. Guevara and L. Glass, J. Math. Biol. **14**, 1 (1982).
[18] F. C. Hoppensteadt and J. Keener, J. Math. Biol. **15**, 339 (1982).
[19] J. Keener and L. Glass, J. Math. Biol. **21**, 175 (1984).
[20] E. J. Ding, Phys. Rev. A **34**, 3547 (1986); E. J. Ding, Phys. Rev. A **35**, 2669 (1987).
[21] W.-Z. Zeng, L. Glass, and A. Shrier, J. Biol. Rhythms **7** 89 (1992).
[22] N. Kopell and L. N. Howard, Studies in Appl. Math. **52**, 291 (1973).
[23] J. W. Milnor, *Topology from the Differentiable Viewpoint* (University Press of Virginia, Charlottesville, 1965), pp. 14 and 15.

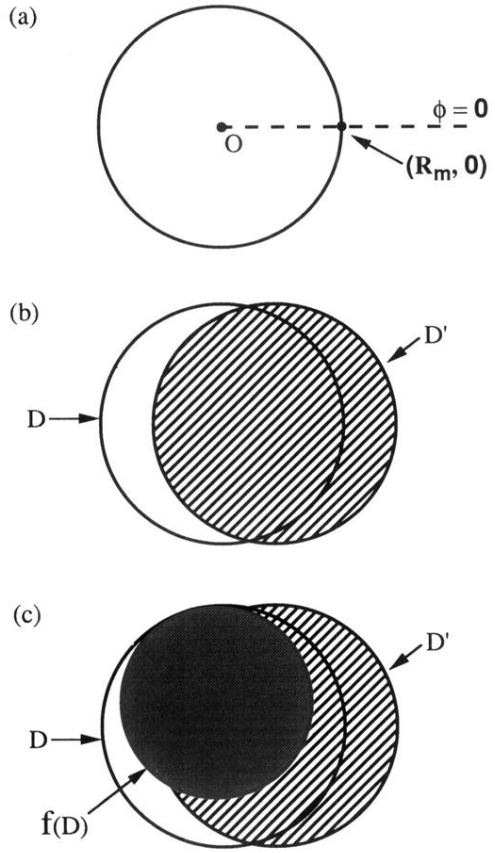

FIG. 3. Schematic diagram showing application of the Brouwer fixed point theorem to prove existence of a period-1 fixed point illustrated for the case $b = 0.8, k = 1.0, \tau = 0.3$. (a) The initial disk D of radius $R_m \approx 1.86$, centered at the origin. (b) D is mapped to a new disk D' by the perturbation of a horizontal translation b. (c) After time τ has elapsed, D evolves to $f(D)$, where $f(D) \in D$.